



**QUEEN'S
UNIVERSITY
BELFAST**

User association and power control in cell-free massive MIMO with the APG method

Hao, C., Vu, T. T., Ngo, H. Q., Dao, M. N., Dang, X., & Matthaiou, M. (2023). User association and power control in cell-free massive MIMO with the APG method. In *Proceedings of the 31st European Signal Processing Conference, EUSIPCO 2023* (pp. 1469-1473). (EUSIPCO Proceedings). Institute of Electrical and Electronics Engineers Inc.. <https://doi.org/10.23919/EUSIPCO58844.2023.10289821>

Published in:

Proceedings of the 31st European Signal Processing Conference, EUSIPCO 2023

Document Version:

Peer reviewed version

Queen's University Belfast - Research Portal:

[Link to publication record in Queen's University Belfast Research Portal](#)

Publisher rights

Copyright 2023 IEEE.

This work is made available online in accordance with the publisher's policies. Please refer to any applicable terms of use of the publisher.

General rights

Copyright for the publications made accessible via the Queen's University Belfast Research Portal is retained by the author(s) and / or other copyright owners and it is a condition of accessing these publications that users recognise and abide by the legal requirements associated with these rights.

Take down policy

The Research Portal is Queen's institutional repository that provides access to Queen's research output. Every effort has been made to ensure that content in the Research Portal does not infringe any person's rights, or applicable UK laws. If you discover content in the Research Portal that you believe breaches copyright or violates any law, please contact openaccess@qub.ac.uk.

Open Access

This research has been made openly available by Queen's academics and its Open Research team. We would love to hear how access to this research benefits you. – Share your feedback with us: <http://go.qub.ac.uk/oa-feedback>

User Association and Power Control in Cell-Free Massive MIMO with the APG Method

Chongzheng Hao^{*†}, Tung T. Vu^{*§}, Hien Quoc Ngo^{*}, Minh N. Dao[‡], Xiaoyu Dang[†], and Michail Matthaiou^{*}

^{*}Centre for Wireless Innovation (CWI), Queen's University Belfast, Belfast, U.K.

[†]College of Electronic and Information Engineering, Nanjing University of Aeronautics and Astronautics, Nanjing, China

[‡]School of Science, RMIT University, Melbourne, VIC 3000, Australia

[§]Department of Electrical Engineering (ISY), Linköping University, Linköping, Sweden

Email: {chongzheng.hao, hien.ngo, m.matthaiou}@qub.ac.uk, thanh.tung.vu@liu.se, minh.dao@rmit.edu.au, dang@nuaa.edu.cn

Abstract—This work proposes a novel approach that jointly designs user equipment (UE) association and power control in a downlink user-centric cell-free massive multiple-input multiple-output (CFmMIMO) network, where each access point (AP) only serves only a set of its associated UEs for reducing the backhaul signaling and computational complexity. Aiming at maximizing the sum spectral efficiency (SE) of the UEs, we formulate a mixed-integer nonconvex optimization problem with quality-of-service and power constraints. Then, we propose a novel accelerated projected gradient (APG) algorithm to obtain a suboptimal solution to the formulated problem. The proposed algorithm is suitable for large-scale CFmMIMO systems with low complexity. Numerical results show that the 50%-likely SE of the proposed method is up to about 2.8 fold higher than that of the heuristic baseline scheme. The APG approach is confirmed to run much faster than the successive convex approximation (SCA) algorithm while obtaining a SE performance close to the SCA approach.

Index Terms—Cell-free massive MIMO, user association, power control, accelerated projected gradient (APG)

I. INTRODUCTION

CFmMIMO has been considered as a promising solution for future generations of communication systems due to its potential to provide handover-free and uniformly good services to all users [1], [2]. In a CFmMIMO system, a large number of APs serve a large number of UEs in the same time and frequency resources. Since CFmMIMO offers high macro-diversity gains along with favorable propagation and channel hardening, it can achieve very high coverage, spectral and energy efficiencies with simplified resource allocation [3], [4]. However, canonical CFmMIMO requires all the APs to serve all the UEs, which makes its implementation difficult in a large-scale system.

To make CFmMIMO more scalable, user-centric CFmMIMO is the most compatible architecture [5], [6]. In a user-centric CFmMIMO system, each AP only needs to receive data and process signals related to its associated UEs. Consequently, the backhaul signaling load and signal processing complexity at

The work of T. T. Vu and H. Q. Ngo was supported by the U.K. Research and Innovation Future Leaders Fellowships under Grant MR/X010635/1. The work of T. T. Vu was also supported partially by the KAW Foundation and by ELLIIT. The work of X. Dang was supported partially by the National Natural Science Foundation of China under Grants 61971221 and 62031017. The work of C. Hao was supported by China Scholarship Council under Grant 202106830001. The work of M. N. Dao was partially supported by the Australian Research Council (ARC), project number DP230101749 and by a public grant as part of the Investissement d'avenir project, reference ANR-11-LABX-0056-LMH, LabEx LMH. The work of M. Matthaiou was supported by the European Research Council (ERC) under the European Union's Horizon 2020 research and innovation program (grant agreement No. 101001331).

each AP can be significantly reduced. User association or/and power control optimization problems of CFmMIMO have been widely discussed in previous literature [7]–[11]. However, no current works have explored low-complexity approaches for joint user association and power control in a large-scale user-centric CFmMIMO system.

In [7], the authors derived the downlink power control algorithm in a user-centric CFmMIMO system and adopted the alternating optimization method to maximize the minimum user's signal to noise and interference ratio (SINR) or the system sum-rate. In [8], the SCA was presented for the energy efficiency maximization with zero-forcing precoding. The authors introduced the second-order Taylor approximation to solve the pilot power control problem for CFmMIMO in [9]. In [10], the authors investigated the max-min fairness power control problem based on the derived downlink achievable rate expression of CFmMIMO and adopted the SCA approach to address the problem. In [11], a user association method was presented using the Hungarian algorithm to maximize the uplink sum rate in the CFmMIMO system. Most of the mentioned works focus on power control or user association. Moreover, the above algorithms require substantial computational resources, thus, making them less likely to be implemented in large-scale CFmMIMO systems.

We herein consider the joint user association and power control for the downlink user-centric CFmMIMO system with the local partial protective zero-forcing (PPZF) processing. We formulate a mixed-integer nonconvex problem for maximizing the achievable sum SE. We, then, propose an APG algorithm to solve the formulated problem with a suboptimal solution. The APG approach has lower complexity than the conventional SCA-based methods and is more suitable for large-scale user-centric CFmMIMO systems. Numerical results confirm that the proposed joint optimization method significantly improves the SE compared to the heuristic approaches. Moreover, the APG algorithm offers a SE performance close to the SCA algorithm while performing considerably faster than the SCA in large-scale CFmMIMO systems.

II. SYSTEM MODEL

We consider a downlink CFmMIMO system, where M APs serve K single-antenna UEs in the same frequency band using time-division duplexing [3]. Each AP is connected to the central processing units (CPUs) via backhaul links and is equipped

with N antennas. Each coherence block includes two phases: uplink training for channel estimation and downlink payload data transmission.

A. Uplink Channel Estimation

In each coherence block of length τ_c symbols, all the UEs send their pilots of length τ_p symbols to the APs simultaneously. We assume that the pilots are pairwise orthogonal, which requires $\tau_p \geq K$. Denote by $\mathbf{g}_{mk} = (\beta_{mk})^{1/2} \tilde{\mathbf{g}}_{mk} \in \mathbb{C}^{N \times 1}$ the channel from UE k to AP m , where $m \in \mathcal{M} \triangleq \{1, \dots, M\}$, $k \in \mathcal{K} \triangleq \{1, \dots, K\}$, β_{mk} and $\tilde{\mathbf{g}}_{mk} \sim \mathcal{CN}(\mathbf{0}, \mathbf{I}_N)$ represent the large-scale fading and small-scale fading coefficients, respectively. At AP m , \mathbf{g}_{mk} is estimated by using the received pilot signals together with the minimum mean-square error (MMSE) estimation technique. By following [3], we can obtain the MMSE estimate of \mathbf{g}_{mk} as $\hat{\mathbf{g}}_{mk}$ which is distributed according to $\mathcal{CN}(\mathbf{0}, \sigma_{mk}^2 \mathbf{I}_N)$, where $\sigma_{mk}^2 = \frac{\tau_p \rho_p \beta_{mk}^2}{\tau_p \rho_p \beta_{mk} + 1}$ and ρ_p is the normalized pilot power at each UE. Let $\hat{\mathbf{G}}_m \triangleq [\hat{\mathbf{g}}_{m1}, \dots, \hat{\mathbf{g}}_{mK}]$ be the estimate of the channel matrix between all the UEs and AP m .

B. Downlink Data Transmission with PPZF Precoding

The APs transmit data to the UEs in the remaining $(\tau_c - \tau_p)$ symbols of each coherence block. In this work, the downlink transmission includes two steps: (S1) precoding design at each AP for all the UEs and (S2) joint UE association and power control for optimizing the SE of the system.

1) *Step (S1)*: Let s_k , where $\mathbb{E}\{|s_k|^2\} = 1$, be the data symbol intended for UE k , where $\mathbb{E}\{\cdot\}$ denotes the statistical expectation. Since the local PPZF processing technique is confirmed to provide a higher SE than the other processing techniques, such as maximum-ratio transmission (MRT), local full-pilot ZF (FZF), and local partial ZF [4], we assume that each AP uses the PPZF processing technique for precoding the downlink signals. The key idea of this technique is that each AP suppresses only the interference that causes to the *strongest* UEs, which have the largest channel gains, while tolerating the interference that causes to the *weakest* UEs. To this end, AP m with PPZF first categorizes the subsets of strong and weak UEs as $\mathcal{S}_m \subset \mathcal{K}$ and $\mathcal{W}_m \subset \mathcal{K}$, respectively. Here, $\mathcal{S}_m \cap \mathcal{W}_m = \emptyset$ and $|\mathcal{S}_m| + |\mathcal{W}_m| = K$, where $|\mathcal{S}|$ is the cardinality of set \mathcal{S} . The strategy for choosing these subsets is discussed later in Section IV. Then, each AP m uses the local PZF technique to precode signals for UEs in \mathcal{S}_m , and uses a protective MRT (PMRT) technique to serve the UEs in \mathcal{W}_m . Specifically, the signal transmitted by AP m is given by $\mathbf{x}_m^{\text{PPZF}} = \sum_{k \in \mathcal{S}_m} \sqrt{\rho_d} \theta_{mk} \mathbf{u}_{mk}^{\text{PZF}} s_k + \sum_{\ell \in \mathcal{W}_m} \sqrt{\rho_d} \theta_{m\ell} \mathbf{u}_{m\ell}^{\text{PMRT}} s_\ell$, where $\mathbf{u}_{mk}^{\text{PZF}} \in \mathbb{C}^{N \times 1}$ and $\mathbf{u}_{m\ell}^{\text{PMRT}} \in \mathbb{C}^{N \times 1}$ are the precoding vectors with $\mathbb{E}\{\|\mathbf{u}_{mk}^{\text{PZF}}\|^2\} = \mathbb{E}\{\|\mathbf{u}_{m\ell}^{\text{PMRT}}\|^2\} = 1$, while ρ_d is the maximum normalized transmit power at each AP and

$$\theta_{mk} \geq 0, \forall m, k, \quad (1)$$

are power control coefficients. The transmitted power at AP m is constrained by $\mathbb{E}\{\|\mathbf{x}_m^{\text{PPZF}}\|^2\} \leq \rho_d$ which is equivalent to

$$\sum_{k \in \mathcal{K}} \theta_{mk}^2 \leq 1, \forall m. \quad (2)$$

Let $\hat{\mathbf{G}}_{\mathcal{S}_m} \in \mathbb{C}^{N \times |\mathcal{S}_m|}$ be the matrix formed by stacking the estimated channels of all UEs in \mathcal{S}_m of AP m . Denote by $j_{mk} \in \{1, \dots, |\mathcal{S}_m|\}$ the index of UE k in \mathcal{S}_m . Then, we have $\hat{\mathbf{G}}_{\mathcal{S}_m} \mathbf{e}_{j_{mk}} = \hat{\mathbf{g}}_{mk}$, where $\mathbf{e}_{j_{mk}}$ is the j_{mk} -th column of $\mathbf{I}_{|\mathcal{S}_m|}$. We note that the set \mathcal{S}_m is independent of the user association. The precoding vector $\mathbf{u}_{mk}^{\text{PZF}}$ is defined as $\mathbf{u}_{mk}^{\text{PZF}} = \sqrt{\sigma_{mk}^2 (N - |\mathcal{S}_m|)} \hat{\mathbf{G}}_{\mathcal{S}_m} (\hat{\mathbf{G}}_{\mathcal{S}_m}^H \hat{\mathbf{G}}_{\mathcal{S}_m})^{-1} \mathbf{e}_{j_{mk}}$ [4], which requires $N > |\mathcal{S}_m|$, while $(\cdot)^H$ stands for the Hermitian transpose. To fully protect the strongest UEs in \mathcal{S}_m from the interference from the weakest UEs in \mathcal{W}_m , the PPZF technique forces the MRT precoded signals of UEs in \mathcal{W}_m to take place in the orthogonal complement of $\hat{\mathbf{G}}_{\mathcal{S}_m}$. Let $\mathbf{B}_m = \mathbf{I}_M - \hat{\mathbf{G}}_{\mathcal{S}_m} (\hat{\mathbf{G}}_{\mathcal{S}_m}^H \hat{\mathbf{G}}_{\mathcal{S}_m})^{-1} \hat{\mathbf{G}}_{\mathcal{S}_m}^H$ be the projection matrix onto the orthogonal complement of $\hat{\mathbf{G}}_{\mathcal{S}_m}$. Then, the PMRT precoding vector for UE ℓ at AP m is $\mathbf{u}_{m\ell}^{\text{PMRT}} = \frac{\mathbf{B}_m \hat{\mathbf{G}}_m \mathbf{e}_\ell}{\sqrt{\sigma_{m\ell}^2 (N - |\mathcal{S}_m|)}}$, where \mathbf{e}_ℓ is the ℓ -th column of \mathbf{I}_M . Here, $\hat{\mathbf{g}}_{mk}^H \mathbf{B}_m = \mathbf{0}^T$ if $k \in \mathcal{S}_m$.

At UE k , the received signal is

$$y_k = \sum_{m \in \mathcal{M}} \mathbf{g}_{mk}^H \mathbf{x}_m + n_k, \quad (3)$$

where $n_k \sim \mathcal{CN}(0, 1)$ is the additive noise. Using the use-and-then-forget capacity-bounding technique, the achievable SE of the system is given by [4, Eq. (33)]

$$\text{SE}_k(\boldsymbol{\theta}) = \frac{\tau_c - \tau_p}{\tau_c} \log_2 \left(1 + \frac{(U_k(\boldsymbol{\theta}))^2}{V_k(\boldsymbol{\theta})} \right), \forall k, \quad (4)$$

where $V_k(\boldsymbol{\theta}) \triangleq \sum_{\ell \in \mathcal{K}} \sum_{m \in \mathcal{M}} \rho_d \theta_{m\ell}^2 (\beta_{mk} - \delta_{mk} \sigma_{mk}^2) + 1$, $U_k(\boldsymbol{\theta}) \triangleq \sum_{m \in \mathcal{M}} \sqrt{\rho_d (N - |\mathcal{S}_m|) \sigma_{mk}^2} \theta_{mk}$, $\boldsymbol{\theta} \triangleq [\theta_1^T, \dots, \theta_M^T]^T$, $\boldsymbol{\theta}_m \triangleq [\theta_{m1}, \dots, \theta_{mK}]^T$, $\delta_{mk} = 1$ if AP m use PZF for UE $k \in \mathcal{S}_m$, and $\delta_{mk} = 0$ if AP m use PMRT for UE $k \in \mathcal{W}_m$. Note that $(\cdot)^T$ denotes the transpose. Here, the SE of each UE needs to be larger than a threshold SE_{QoS}

$$\text{SE}_k(\boldsymbol{\theta}) \geq \text{SE}_{\text{QoS}}, \forall k. \quad (5)$$

2) *Step (S2)*: In a practical large-scale CFmMIMO system with a large value of K , the backhaul signal load to each AP should be limited, and the number of UEs served by each AP should be restricted by a number smaller than K to reduce the complexity at each AP [5]. This also means that each UE is only served by a set of its associated APs instead of all the APs. The association of UE k and AP m is defined as

$$a_{mk} \triangleq \begin{cases} 1, & \text{if UE } k \text{ associates with AP } m \\ 0, & \text{otherwise} \end{cases}, \forall m, k. \quad (6)$$

We have

$$(\theta_{mk}^2 = 0, \forall k, \text{ if } a_{mk} = 0), \quad \forall m, \quad (7)$$

to guarantee that if AP m does not associate with UE k , the transmit power $\rho_d \theta_{mk}^2$ towards UE k is zero. Note that since Steps (S1) and (S2) are performed separately, the UE association in this step does not affect the precoding signals in Step (S1) and the mathematical structure of SE_k in (4). The UE association variable a_{mk} only affects SE_k via power θ_{mk}^2 and (7). Here, we have

$$\sum_{k \in \mathcal{K}} a_{mk} \text{SE}_k(\boldsymbol{\theta}) \leq C_{\max, m}, \forall m, \quad (8)$$

$$\sum_{k \in \mathcal{K}} a_{mk} \leq \hat{K}_m, \forall m, \quad (9)$$

$$\sum_{m \in \mathcal{M}} a_{mk} \geq 1, \forall k, \quad (10)$$

to guarantee that the backhaul load at each AP m is below a threshold $C_{\max, m}$, the maximum number of UEs served by each AP m is \widehat{K}_m , and each UE is served by at least one AP.

III. PROBLEM FORMULATION AND SOLUTION

A. Problem Formulation

In this section, we aim at optimizing UE association $\mathbf{a} \triangleq \{a_{mk}\}, \forall m, k$, and the power control coefficients $\boldsymbol{\theta}$ to maximize the sum SE. Specifically, we formulate an optimization problem as follows:

$$\begin{aligned} \max_{\mathbf{a}, \boldsymbol{\theta}} \quad & \sum_{k \in \mathcal{K}} \text{SE}_k(\boldsymbol{\theta}) \\ \text{s.t.} \quad & (1), (2), (5) - (10). \end{aligned} \quad (11)$$

Note that (11) is a mixed-integer optimization problem with highly nonconvex constraints, whose solution is challenging to find. Instead, we aim to design algorithms that are suitable for practical implementation.

First, to deal with the binary constraint (6), we see that $x \in \{0, 1\} \Leftrightarrow x \in [0, 1] \& x - x^2 \leq 0$ [12]. Therefore, (6) can be replaced by

$$Q(\mathbf{a}) \triangleq \sum_{k \in \mathcal{K}} \sum_{m \in \mathcal{M}} (a_{mk} - a_{mk}^2) \leq 0, \quad (12)$$

$$0 \leq a_{mk}, \forall m, k, \quad (13)$$

$$a_{mk} \leq 1, \forall m, k. \quad (14)$$

In the light of (2), we replace the constraint (7) by

$$\theta_{mk}^2 \leq a_{mk}, \forall m, k. \quad (15)$$

Problem (11) is now equivalent to

$$\min_{\mathbf{x} \in \mathcal{F}} - \sum_{k \in \mathcal{K}} \text{SE}_k(\boldsymbol{\theta}), \quad (16)$$

where $\mathbf{x} \triangleq \{\mathbf{a}, \boldsymbol{\theta}\}$, $\mathcal{F} \triangleq \{(1), (2), (5), (8) - (10), (12) - (15)\}$ is a feasible set. Problem (16) can be solved using SCA-based algorithms [13].¹ However, such approaches have high complexity and, importantly, a slow running time when the size of the problem is large (i.e., $MK \geq 1000$). Therefore, we propose a low-complexity approach to solve the problem (16) using APG techniques [14], [15].

B. APG Approach

$$\begin{aligned} \text{We first let } z_{mk}^2 &\triangleq a_{mk}, \forall m, k \text{ and} \\ &0 \leq z_{mk} \leq 1, \forall m, k. \end{aligned} \quad (17)$$

Then, (5), (8), (10), (12) and (15) can be replaced by

$$Q_1(\mathbf{z}) \triangleq \sum_{k \in \mathcal{K}} \sum_{m \in \mathcal{M}} (z_{mk}^2 - z_{mk}^4) \leq 0, \quad (18)$$

$$Q_2(\boldsymbol{\theta}) \triangleq \sum_{k \in \mathcal{K}} \left[\max\left(0, \text{SE}_{\text{QoS}} - \text{SE}_k(\boldsymbol{\theta})\right) \right]^2 \leq 0, \quad (19)$$

$$\begin{aligned} Q_3(\boldsymbol{\theta}, \mathbf{z}) &\triangleq \sum_{k \in \mathcal{K}} \left(\left[\max\left(0, 1 - \sum_{m \in \mathcal{M}} z_{mk}^2\right) \right]^2 \right. \\ &\quad \left. + \sum_{m \in \mathcal{M}} [\max(0, \theta_{mk}^2 - z_{mk}^2)]^2 \right) \leq 0, \end{aligned} \quad (20)$$

¹The details of the SCA algorithms to solve (16) are omitted due to lack of space.

Algorithm 1 Solving problem (23) using the APG approach

- 1: **Initialize:** $n = 1$, $q^{(0)} = 0$, $q^{(1)} = 1$, random $\mathbf{v}^{(0)}, \bar{\mathbf{v}}^{(0)} \in \widehat{\mathcal{H}}$, $\alpha_{\bar{\mathbf{v}}} > 0$, $\alpha_{\mathbf{v}} > 0$, $\tilde{\mathbf{v}}^{(1)} = \mathbf{v}^{(1)} = \mathbf{v}^{(0)}$, $\zeta \in [0, 1)$, $b^{(1)} = 1$, $v > 0$, $c^{(1)} = f(\mathbf{v}^{(1)})$, $\Delta > 1$
- 2: **repeat**
- 3: **repeat**
- 4: Update $\bar{\mathbf{v}}^{(n)}$ as (25) and $\tilde{\mathbf{v}}^{(n+1)}$ as (27)
- 5: **if** $f(\tilde{\mathbf{v}}^{(n+1)}) \leq c^{(n)} - \zeta \|\tilde{\mathbf{v}}^{(n+1)} - \bar{\mathbf{v}}^{(n)}\|^2$ **then**
- 6: $\mathbf{v}^{(n+1)} = \tilde{\mathbf{v}}^{(n+1)}$
- 7: **else**
- 8: Update $\hat{\mathbf{v}}^{(n+1)}$ as (30)
- 9: Update $\mathbf{v}^{(n+1)}$ as (31)
- 10: **end if**
- 11: Update $q^{(n+1)}$ as (26)
- 12: Update $b^{(n+1)}$ as (28) and $c^{(n+1)}$ as (29)
- 13: Update $n = n + 1$
- 14: **until** $\left| \frac{f(\mathbf{v}^{(n)}) - f(\mathbf{v}^{(n-1)})}{f(\mathbf{v}^{(n)})} \right| \leq \epsilon$ or $\left| \frac{h(\boldsymbol{\theta}^{(n)}) - h(\boldsymbol{\theta}^{(n-1)})}{h(\boldsymbol{\theta}^{(n)})} \right| \leq \epsilon$
- 15: Increase $\chi = \chi \times \Delta$
- 16: **until** convergence

$$Q_4(\boldsymbol{\theta}, \mathbf{z}) \triangleq \sum_{m \in \mathcal{M}} \left[\max\left(0, \sum_{k \in \mathcal{K}} z_{mk}^2 \text{SE}_k(\boldsymbol{\theta}) - C_{\max, m}\right) \right]^2 \leq 0. \quad (21)$$

Therefore, problem (16) is equivalent to

$$\min_{\mathbf{v}} h(\boldsymbol{\theta}) \triangleq - \sum_{k \in \mathcal{K}} \text{SE}_k(\boldsymbol{\theta}) \quad (22a)$$

$$\text{s.t. } (1), (2), (17) - (21) \quad (22b)$$

$$\sum_{k \in \mathcal{K}} z_{mk}^2 \leq \widehat{K}_m, \forall m, \quad (22c)$$

where (22c) follows (9), $\mathbf{v} \triangleq [\boldsymbol{\theta}^T, \mathbf{z}^T]^T$, $\mathbf{z} \triangleq [z_1^T, \dots, z_M^T]^T$, $\mathbf{z}_m \triangleq [z_{m1}, \dots, z_{mK}]^T$. Let $\mathcal{H} \triangleq \{(1), (2), (17) - (21), (22c)\}$ is the feasible set of (22). We consider the following problem

$$\min_{\mathbf{v} \in \widehat{\mathcal{H}}} f(\mathbf{v}), \quad (23)$$

where $\widehat{\mathcal{H}} \triangleq \{(1), (2), (17), (22c)\}$ is a convex feasible set of (23), $f(\mathbf{v}) \triangleq h(\boldsymbol{\theta}) + \chi [\mu_1 Q_1(\mathbf{z}) + \mu_2 Q_2(\boldsymbol{\theta}) + \mu_3 Q_3(\boldsymbol{\theta}, \mathbf{z}) + \mu_4 Q_4(\boldsymbol{\theta}, \mathbf{z})]$ is the Lagrangian of (22), $\mu_1, \mu_2, \mu_3, \mu_4$ are fixed and positive weights, χ is the Lagrangian multiplier corresponding to constraints (18)–(21).

Proposition 1. *The values $Q_{1,\chi}, Q_{2,\chi}, Q_{3,\chi}, Q_{4,\chi}$ of Q_1, Q_2, Q_3, Q_4 at the solution of (23) corresponding to χ converge to 0 as $\chi \rightarrow +\infty$. Also, problem (22) has strong duality, i.e.,*

$$\min_{\mathbf{v} \in \mathcal{H}} - \sum_{k \in \mathcal{K}} \text{SE}_k(\boldsymbol{\theta}) = \sup_{\chi \geq 0} \min_{\mathbf{v} \in \widehat{\mathcal{H}}} f(\mathbf{v}). \quad (24)$$

Then, (23) is equivalent to (22) at the optimal solution $\chi^ \geq 0$ of the sup-min problem in (24).*

The proof of Proposition 1 follows [13], and hence, is omitted due to lack of space. For practical implementation, it is acceptable for $Q_{1,\chi}/(MK), Q_{2,\chi}/K, Q_{3,\chi}/(MK), Q_{4,\chi}/M \leq \epsilon$, for some small ϵ with a sufficiently large value of χ .

The main steps for solving problem (23) are outlined in Algorithm 1. Starting with a random point $\mathbf{v}^{(0)} \in \widehat{\mathcal{H}}$, we compute an extrapolated point for accelerating the convergence of the algorithm as

$$\bar{\mathbf{v}}^{(n)} = \mathbf{v}^{(n)} + \frac{q^{(n-1)}}{q^{(n)}} (\tilde{\mathbf{v}}^{(n)} - \mathbf{v}^{(n)}) + \frac{q^{(n-1)} - 1}{q^{(n)}} (\mathbf{v}^{(n)} - \mathbf{v}^{(n-1)}), \quad (25)$$

where $q^{(n)}$ is an extrapolation parameter in iteration n and computed recursively as

$$q^{(n+1)} = \frac{1 + \sqrt{4(q^{(n)})^2 + 1}}{2}. \quad (26)$$

From $\bar{\mathbf{v}}^{(n)}$, we move along the gradient of the function with a dedicated step size $\alpha_{\bar{\mathbf{v}}}$. Then, the resulting point $(\bar{\mathbf{v}} - \alpha_{\bar{\mathbf{v}}} \nabla f(\bar{\mathbf{v}}))$ is projected onto the feasible set $\hat{\mathcal{H}}$ to obtain

$$\hat{\mathbf{v}}^{(n+1)} = \mathcal{P}_{\hat{\mathcal{H}}}(\bar{\mathbf{v}}^{(n)} - \alpha_{\bar{\mathbf{v}}} \nabla f(\bar{\mathbf{v}}^{(n)})), \quad (27)$$

where $\mathcal{P}_{\hat{\mathcal{H}}}(\mathbf{y})$ is the operator of projecting \mathbf{y} on $\hat{\mathcal{H}}$. Since $f(\mathbf{v})$ is not convex, $f(\hat{\mathbf{v}}^{(n+1)})$ may not improve the objective sequence, we accept $\mathbf{v}^{(n+1)} = \hat{\mathbf{v}}^{(n+1)}$ if the objective value $f(\hat{\mathbf{v}}^{(n+1)})$ is smaller than $c^{(n)}$ which is a relaxation of $f(\mathbf{v}^{(n)})$ but not far from $f(\mathbf{v}^{(n)})$. Following [15], $c^{(n)} = \frac{\sum_{n=1}^{\kappa} \zeta^{(\kappa-n)} f(\mathbf{v}^{(n)})}{\sum_{n=1}^{\kappa} \zeta^{(\kappa-n)}}$, which is the weighted average of $f(\mathbf{v}^{(n)})$, is chosen, where $\zeta \in [0, 1)$. In each iteration, $c^{(n+1)}$ can be computed by

$$b^{(n+1)} = \zeta b^{(n)} + 1, \quad (28)$$

$$c^{(n+1)} = \frac{\zeta b^{(n)} c^{(n)} + f(\mathbf{v}^{(n)})}{b^{(n+1)}}, \quad (29)$$

where $c^{(1)} = f(\mathbf{v}^{(1)})$ and $b^{(1)} = 1$.

If $f(\hat{\mathbf{v}}^{(n+1)}) \leq c^{(n)} - \zeta \|\hat{\mathbf{v}}^{(n+1)} - \bar{\mathbf{v}}^{(n)}\|^2$ does not hold, additional correction steps are used to prevent this event, where $\|\mathbf{x}\|$ is the Euclidean norm of \mathbf{x} . Specifically, another point

$$\hat{\hat{\mathbf{v}}}^{(n+1)} = \mathcal{P}_{\hat{\mathcal{H}}}(\mathbf{v}^{(n)} - \alpha_{\mathbf{v}} \nabla f(\mathbf{v}^{(n)})), \quad (30)$$

is computed with a dedicated step size $\alpha_{\mathbf{v}}$. Then, we update $\mathbf{v}^{(n+1)}$ by comparing the objective values at $\hat{\mathbf{v}}^{(n+1)}$ and $\hat{\hat{\mathbf{v}}}^{(n+1)}$ as

$$\mathbf{v}^{(n+1)} \triangleq \begin{cases} \hat{\mathbf{v}}^{(n+1)}, & \text{if } f(\hat{\mathbf{v}}^{(n+1)}) \leq f(\hat{\hat{\mathbf{v}}}^{(n+1)}) \\ \hat{\hat{\mathbf{v}}}^{(n+1)}, & \text{otherwise} \end{cases}. \quad (31)$$

Since the feasible set $\hat{\mathcal{H}}$ is bounded, it is true that $\nabla f(\mathbf{v})$ is Lipschitz continuous with an existing value of L , i.e.,

$$\|\nabla f(\mathbf{x}) - \nabla f(\mathbf{y})\| \leq L \|\mathbf{x} - \mathbf{y}\|, \forall \mathbf{x}, \mathbf{y} \in \hat{\mathcal{H}}. \quad (32)$$

In our numerical results, $\alpha_{\bar{\mathbf{v}}}$ and $\alpha_{\mathbf{v}}$ are kept fixed as sufficiently small values and still offer a convergence for the Algorithm 1.

In Algorithm 1, the projection in (27) and (30) is performed by solving the following problem

$$\mathcal{P}_{\hat{\mathcal{H}}}(\mathbf{v}) : \min_{\mathbf{v} \in \mathbb{R}^{2MK \times 1}} \|\mathbf{v} - \mathbf{r}\|^2 \quad (33)$$

$$\text{s.t.} \quad (1), (2), (17), (22c),$$

for any given vector $\mathbf{r} = [\mathbf{r}_1^T, \mathbf{r}_2^T]^T \in \mathbb{R}^{2MK \times 1}$, where $\mathbf{r}_1 \triangleq [\mathbf{r}_{1,1}^T, \dots, \mathbf{r}_{1,M}^T]^T$, $\mathbf{r}_{1,m} \triangleq [r_{1,m1}, \dots, r_{1,mK}]^T$, $\mathbf{r}_2 \triangleq [\mathbf{r}_{2,1}^T, \dots, \mathbf{r}_{2,M}^T]^T$, $\mathbf{r}_{2,m} \triangleq [r_{2,m1}, \dots, r_{2,mK}]^T$. Problem (33) can be decomposed into two separate subproblems of optimizing $\boldsymbol{\theta}_m$ and \mathbf{z}_m for each m as

$$\min_{\boldsymbol{\theta}_m \in \mathbb{R}^{MK \times 1}} \|\boldsymbol{\theta}_m - \mathbf{r}_{1,m}\|^2 \quad (34)$$

$$\text{s.t.} \quad \|\boldsymbol{\theta}_m\|^2 \leq 1, \boldsymbol{\theta}_m \geq 0,$$

$$\min_{\mathbf{z}_m \in \mathbb{R}^{MK \times 1}} \|\mathbf{z}_m - \mathbf{r}_{2,m}\|^2 \quad (35)$$

$$\text{s.t.} \quad \|\mathbf{z}_m\|^2 \leq \hat{K}_m, \mathbf{z}_m \geq 0, \mathbf{z}_m \leq 1,$$

where the constraints in problems (34) and (35) follow (1), (2), (17), (22c). The solution to the problem (34) is the projection of a given point onto the intersection of a Euclidean ball and the positive orthant, which have a closed-form as [14], [15]

$$\boldsymbol{\theta}_m = \frac{1}{\max(1, \|\mathbf{r}_{1,m}\|_{0+})} [\mathbf{r}_{1,m}]_{0+}, \quad (36)$$

where $[\mathbf{x}]_{0+} \triangleq [\max(0, x_1), \dots, \max(0, x_K)]^T, \forall \mathbf{x} \in \mathbb{R}^{K \times 1}$. The solution to problem (35) is the projection of a given point onto the intersection of a Euclidean ball and a box, which can be approximated by

$$\mathbf{z}_m = \left[\frac{\sqrt{\hat{K}_m}}{\max(\sqrt{\hat{K}_m}, \|\mathbf{r}_{2,m}\|_{0+})} [\mathbf{r}_{2,m}]_{0+} \right]_{1-}, \quad (37)$$

where $[\mathbf{x}]_{1-} \triangleq [\min(1, x_1), \dots, \min(1, x_K)]^T, \forall \mathbf{x} \in \mathbb{R}^{K \times 1}$. Note that the solution (37) is not yet the optimal solution to problem (35) but is close to this solution.

The values of $\frac{\partial}{\partial \theta_{mk}} f(\mathbf{v})$ and $\frac{\partial}{\partial z_{mk}} f(\mathbf{v})$ are computed by

$$\frac{\partial}{\partial \theta_{mk}} f(\mathbf{v}) = - \sum_{i \in \mathcal{K}} \frac{\partial}{\partial \theta_{mk}} \text{SE}_i(\mathbf{v}) + \chi \frac{\partial}{\partial \theta_{mk}} \tilde{Q}(\mathbf{v}), \quad (38)$$

$$\frac{\partial}{\partial z_{mk}} f(\mathbf{v}) = - \sum_{i \in \mathcal{K}} \frac{\partial}{\partial z_{mk}} \text{SE}_i(\mathbf{v}) + \chi \frac{\partial}{\partial z_{mk}} \tilde{Q}(\mathbf{v}), \quad (39)$$

where

$$\frac{\partial}{\partial \theta_{mk}} \text{SE}_i(\mathbf{v}) = \frac{\tau_c - \tau_p}{\tau_c \log 2} \left[\frac{\frac{\partial}{\partial \theta_{mk}} (U_i(\mathbf{v}) + V_i(\mathbf{v}))}{(U_i(\mathbf{v}) + V_i(\mathbf{v}))} - \frac{\frac{\partial}{\partial \theta_{mk}} V_i(\mathbf{v})}{V_i(\mathbf{v})} \right], \quad (40)$$

$$\frac{\partial}{\partial z_{mk}} \text{SE}_i(\mathbf{v}) = \frac{\tau_c - \tau_p}{\tau_c \log 2} \left[\frac{\frac{\partial}{\partial z_{mk}} (U_i(\mathbf{v}) + V_i(\mathbf{v}))}{(U_i(\mathbf{v}) + V_i(\mathbf{v}))} - \frac{\frac{\partial}{\partial z_{mk}} V_i(\mathbf{v})}{V_i(\mathbf{v})} \right]. \quad (41)$$

Here, $\frac{\partial}{\partial z_{mk}} U_i(\mathbf{v}) = 0, \frac{\partial}{\partial z_{mk}} V_i(\mathbf{v}) = 0, \forall m, k, i$,

$$\frac{\partial}{\partial \theta_{mk}} U_i(\mathbf{v}) = \begin{cases} \left(\sum_{m \in \mathcal{M}} \sqrt{\rho_d(N - |\mathcal{S}_m|) \sigma_{mk}^2} \theta_{mk} \right) \\ \times 2 \times \sqrt{\rho_d(N - |\mathcal{S}_m|) \sigma_{mk}^2}, & i = k, \\ 0, & i \neq k \end{cases} \quad (42)$$

$$\frac{\partial}{\partial \theta_{mk}} V_i(\mathbf{v}) = \begin{cases} 2\rho_d(\beta_{mk} - \delta_{mk} \sigma_{mk}^2) \theta_{mk}, & i = k \\ 2\rho_d(\beta_{mi} - \delta_{mi} \sigma_{mi}^2) \theta_{mk}, & i \neq k \end{cases}. \quad (43)$$

From the definitions of Q_1, Q_2, Q_3, Q_4 in (18)–(21), we have

$$\begin{aligned} \frac{\partial}{\partial \theta_{mk}} \tilde{Q}(\mathbf{v}) &= \mu_3 4 \max(0, \theta_{mk}^2 - z_{mk}^2) \theta_{mk} \\ &- \mu_2 \sum_{i \in \mathcal{K}} 2 \max(0, \text{SE}_{QoS} - \text{SE}_i(\boldsymbol{\theta})) \frac{\partial}{\partial \theta_{mk}} \text{SE}_i(\mathbf{v}) + \mu_4 \times \\ &\sum_{i \in \mathcal{K}} 2 \max(0, \sum_{i \in \mathcal{K}} z_{mi}^2 \text{SE}_i(\boldsymbol{\theta}) - C_{\max, m}) z_{mi}^2 \frac{\partial}{\partial \theta_{mk}} \text{SE}_i(\mathbf{v}), \quad (44) \\ \frac{\partial}{\partial z_{mk}} \tilde{Q}(\mathbf{v}) &= \mu_1 (2z_{mk} - 4z_{mk}^3) - \mu_3 4 \max(0, \theta_{mk}^2 - z_{mk}^2) z_{mk} \\ &- \mu_3 4 \max(0, 1 - \sum_{m \in \mathcal{M}} z_{mk}^2) z_{mk} \\ &+ \mu_4 4 \max(0, \sum_{i \in \mathcal{K}} z_{mi}^2 \text{SE}_i(\boldsymbol{\theta}) - C_{\max, m}) z_{mk} \text{SE}_k(\mathbf{v}). \quad (45) \end{aligned}$$

In each iteration, the APG-based Algorithm 1 only requires computing the gradient and projecting a point into the feasible $\hat{\mathcal{H}}$ with closed-form solutions, while the SCA requires solving an optimization problem. Therefore, the complexity of each iteration of Algorithm 1 is expected to be much lower than that of the SCA approach for given the same large-scale system.

IV. NUMERICAL EXAMPLES

We consider a CFmMIMO network, where the APs and UEs are randomly located in a square of 1×1 km². The distances

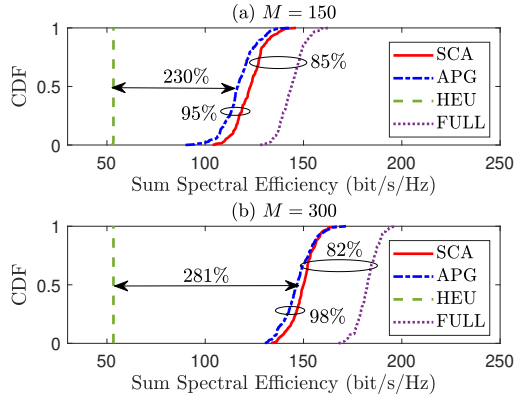


Fig. 1. Comparison among the considered schemes ($K = 40$).

between adjacent APs are at least 50 m. We set $N = 2$, $\tau_c = 200$ samples, $\hat{K}_m = \hat{K} = 15$, $C_{\max, m} = C_{\max} = 20$ bit/s/Hz, $\forall m$. The large-scale fading coefficients, β_{mk} , are modeled in the same manner as [16, Eqs. (37), (38)]. Let $\tilde{\rho}_d = 1$ W and $\tilde{\rho}_p = 0.1$ W be the maximum transmit power of the APs and uplink pilot symbols, respectively. The maximum transmit powers ρ_d and ρ_p are normalized by the noise power. Each AP m chooses its subset \mathcal{S}_m by selecting the UEs that contribute at least $\mu\%$ of the overall channel gain [4], while μ is adjusted to guarantee $N > |\mathcal{S}_m|$. In the algorithms, we set $\Delta = 2$, $\chi = 1$, $\alpha_{\bar{v}} = \alpha_v = 10^{-4}$, $\zeta = 10^{-1}$, and $v = 10^{-2}$.

To evaluate the effectiveness of our proposed schemes, we consider the following baseline schemes: 1) **SCA**: We transform the problem (16) into a tractable form and jointly optimize \mathbf{a} and $\boldsymbol{\theta}$ using the SCA algorithm; 2) **Full UE association (FULL)**: All the UEs are served by all the AP, without constraints (8)–(10). We then apply our algorithm to optimize the power control coefficients $\boldsymbol{\eta}$; 3) **Heuristic UE association (HEU)**: First, each UE is associated to the AP that has the strongest gains to guarantee (10). After this step, let κ_m be the number of UEs that are associated to AP m . To guarantee (9), each AP m fills up its set of \hat{K} UEs to serve by selecting $(\hat{K} - \kappa_m)$ UEs that have the strongest channel gains. Finally, $\boldsymbol{\eta}$ is optimized similarly as **FULL**.

Note that the UE association approaches discussed in [7]–[11] do not consider the maximum number of UEs served by one AP in (9) as well as the maximum backhaul signaling load, and hence, are not compared with our proposed approaches.

Figure 1 compares the SE of all the considered schemes. As seen, in terms of 50%-likely performance (median value) of sum SE, our proposed **APG** schemes significantly outperform the heuristic scheme **HEU**. In particular, **APG** increases the 50%-likely sum SE by substantial amounts compared with that of **HEU**, e.g., by up to 230% with $M = 150$ and 281% with $M = 300$. Moreover, the sum SEs of **SCA** and **APG** are close to that of **FULL**, i.e., up to 82% with $M = 300$. These results show the significant advantage of joint optimization of UE association and power control to improve the SE of user-centric CFmMIMO systems. As also seen from Fig. 1, **APG** can provide a sum SE that is close to that of **SCA**. The 50%-likely sum SE of **APG** can approach up to 95% and 98% that of **SCA** with $M = 150$ and $M = 300$, respectively. On the other

TABLE I

| MK | Average running time ratio of SCA over APG |
|-------|--|
| 6000 | ≈ 12.63 fold |
| 12000 | ≈ 15.21 fold |

hand, **APG** is implemented much faster than **SCA** as shown in Table I. The average running time of **APG** is up to 15.21 fold smaller than that of **SCA** when $MK = 12000$.

V. CONCLUSION

We have proposed a joint optimization approach of UE association and power control for CFmMIMO. We formulated a mixed-integer nonconvex optimization problem to maximize the sum SE and presented a novel **APG** approach to solve the considered problem. Numerical results showed that the presented **APG** algorithm can significantly increase the SE compared with the heuristic approaches and obtain nearly the same SE as the **SCA** method with considerably lower complexity.

REFERENCES

- [1] M. Matthaiou, O. Yurduseven, H. Q. Ngo, D. Morales-Jimenez, S. L. Cotton, and V. F. Fusco, "The road to 6G: Ten physical layer challenges for communications engineers," *IEEE Commun. Mag.*, vol. 59, no. 1, pp. 64–69, Jan. 2021.
- [2] J. Zhang, E. Björnson, M. Matthaiou, D. W. K. Ng, H. Yang, and D. J. Love, "Prospective multiple antenna technologies for beyond 5G," *IEEE J. Select. Areas Commun.*, vol. 38, no. 8, pp. 1637–1660, Aug. 2020.
- [3] H. Q. Ngo, A. Ashikhmin, H. Yang, E. G. Larsson, and T. L. Marzetta, "Cell-free massive MIMO versus small cells," *IEEE Trans. Wireless Commun.*, vol. 16, no. 3, pp. 1834–1850, Mar. 2017.
- [4] G. Interdonato, M. Karlsson, E. Björnson, and E. G. Larsson, "Local partial zero-forcing precoding for cell-free massive MIMO," *IEEE Trans. Wireless Commun.*, vol. 19, no. 7, pp. 4758–4774, Jul. 2020.
- [5] Ö. T. Demir, E. Björnson, and L. Sanguinetti, *Foundations of User-Centric Cell-Free Massive MIMO*. Foundations and Trends in Signal Processing, 2021, vol. 14, no. 3-4.
- [6] M. Alonzo, S. Buzzi, A. Zappone, and C. D'Elia, "Energy-efficient power control in cell-free and user-centric massive MIMO at millimeter wave," *IEEE Trans. Green Commun. Networking*, vol. 3, no. 3, pp. 651–663, Mar. 2019.
- [7] S. Buzzi and A. Zappone, "Downlink power control in user-centric and cell-free massive MIMO wireless networks," in *Proc. IEEE PIMRC*, Oct. 2017, pp. 1–6.
- [8] L. D. Nguyen, T. Q. Duong, H. Q. Ngo, and K. Tourki, "Energy efficiency in cell-free massive MIMO with zero-forcing precoding design," *IEEE Commun. Lett.*, vol. 21, no. 8, pp. 1871–1874, Apr. 2017.
- [9] T. C. Mai, H. Q. Ngo, M. Egan, and T. Q. Duong, "Pilot power control for cell-free massive MIMO," *IEEE Trans. Veh. Technol.*, vol. 67, no. 11, pp. 11 264–11 268, Aug. 2018.
- [10] G. Interdonato, H. Q. Ngo, P. Frenger, and E. G. Larsson, "Downlink training in cell-free massive MIMO: A blessing in disguise," *IEEE Trans. Wireless Commun.*, vol. 18, no. 11, pp. 5153–5169, Aug. 2019.
- [11] C. D'Andrea and E. G. Larsson, "User association in scalable cell-free massive MIMO systems," in *Proc. IEEE ASILOMAR*, Nov. 2020, pp. 826–830.
- [12] T. T. Vu, D. T. Ngo, H. Q. Ngo, M. N. Dao, N. H. Tran, and R. H. Middleton, "Joint resource allocation to minimize execution time of federated learning in cell-free massive MIMO," *IEEE Internet Things J.*, vol. 9, no. 21, pp. 21 736–21 750, Jun. 2022.
- [13] T. T. Vu, D. T. Ngo, M. N. Dao, S. Durrani, and R. H. Middleton, "Spectral and energy efficiency maximization for content-centric C-RANs with edge caching," *IEEE Trans. Commun.*, vol. 66, no. 12, pp. 6628–6642, Dec. 2018.
- [14] M. Farooq, H. Q. Ngo, E.-K. Hong, and L.-N. Tran, "Utility maximization for large-scale cell-free massive MIMO downlink," *IEEE Trans. Commun.*, vol. 69, no. 10, pp. 7050–7062, Oct. 2021.
- [15] H. Li and Z. Lin, "Accelerated proximal gradient methods for nonconvex programming," in *Proc. Int. Conf. Neural Inform. Process. Syst. (NIPS)*, vol. 28, Dec. 2015, pp. 379–387.
- [16] E. Björnson and L. Sanguinetti, "Making cell-free massive MIMO competitive with MMSE processing and centralized implementation," *IEEE Trans. Wireless Commun.*, vol. 19, no. 1, pp. 77–90, Jan. 2020.